

OMAE2008-57882

Centerwell Water Motions and Hydrodynamic Loading Using Viscous Flow Calculations

Samuel Holmes
Red Wing Engineering, Inc.

Joseph Gebara
Technip

Allan Magee
Technip

ABSTRACT

Most Spar platforms have a wet centerwell which provides a termination point for umbilicals and risers. The column of water in the centerwell is a dynamic system which can be excited by the wave action around the Spar as well as the platform's own motions. When the exciting frequencies are close to the natural frequency of the water column, the vertical motion of the water in the centerwell can become large in large seastates. This might damage structures within the centerwell. A natural response to this problem is to restrict the fluid flow at the bottom of the centerwell by adding a plated structure to partially close the opening. The remaining open area in the centerwell determines the amount of damping as well as the loads on the plating which can be quite large in heavy seas. The problem addressed in this paper is the determination of the appropriate open area in the centerwell plate that will control the fluid vertical motion without requiring expensive reinforcements to the plating beyond the riser guide structure already present. Traditional design tools based on potential flow models appear to perform poorly for this problem because they do not model the viscous damping in the flow correctly. In this paper we use a Navier-Stokes solver to study the centerwell motions and centerwell plate loads for three centerwell plate geometries. It is found that the Spar motions and the free surface waves need to be included in these simulations. The centerwell water motions and centerwell plate loads are compared with those measured in a scale model experiment. Full-scale calculations are also carried out to determine the corresponding centerwell plate loads and centerwell water motions to assess scale effects.

NOMENCLATURE

a = centerwell water motion amplitude (m)

h = centerwell water motion height (peak to trough) (m)

g = acceleration of gravity

A = centerwell cross section area (m²)

H = incident wave height, regular waves (m)

H_s = significant wave height, random waves (m)

L = centerwell height

z = centerwell depth from mean waterline (m)

$Re = UD/\nu$ = Reynolds number

t = time [s]

U = current velocity [m/s]

x, y, z = coordinates

ρ = density (kg/m³)

ω = frequency (rad/s)

INTRODUCTION

The risers on early Spars were typically attached to buoyancy cans which effectively blocked much of the centerwell inlet area. Centerwell water motions were usually not a concern. Some newer Spar designs have a more open centerwell leading to increased centerwell water motions. This type of design is illustrated in Figure 1. In this design, structural members and supports for riser guides are typically placed at the bottom of the hard tank. Additional plating over these guide structures forms a structure that can be used to dampen the centerwell water column motion. Larger centerwell plate coverage decreases the centerwell water column motion but leads to increased loads on the plating structure, requiring expensive reinforcements. The practical design issue then is to determine the centerwell plating arrangement that sufficiently dampens the centerwell water motions without unduly increasing the loads on the plate.



Figure 1. Spar platform. Note centerwell opening, centerwell plate and upper heave plate.

Assuming small displacements without friction and with a uniform velocity distribution, the column of water in the centerwell has a natural frequency that depends only on the column height. Assuming that the column behaves as a simple harmonic oscillator with small displacements and negligible damping, the maximum potential energy of the column is:

$$PE_{\max} = \frac{1}{2} \rho g A a^2$$

where a is the vibration amplitude. The maximum kinetic energy is

$$KE_{\max} = \frac{1}{2} \rho L A a^2 \omega^2$$

Equating the maximum kinetic energy with the maximum potential energy we obtain:

$$\omega = \sqrt{\frac{g}{L}}$$

Thus for a centerwell height of 60m the natural period of vibration of the column of water is about 15.5 seconds, right in the middle of the range of wave periods used to characterize sea conditions in heavy seas.

In order to design the plate at the bottom of the centerwell, we chose a design approach in which the centerwell open area is varied and CFD simulations are used to find the effects on centerwell water column motions and centerwell plate loads. We expect viscous effects may be important in this problem for several reasons. One of these is that the opening in the centerwell is subjected to significant unsteady flow in all directions due to wave induced motions and the interaction of the flow with the hard tank. Thus, large eddies inside and outside of the centerwell may affect the flow. This might be expected from the observations of those designing buildings for ventilation in unsteady air flows. For example, Chiu and Etheridge [1] have shown that static discharge coefficients are not appropriate for building openings under these conditions. The same reasoning suggests that scale or Reynolds number effects may be more important than they are in determining static discharge coefficients.

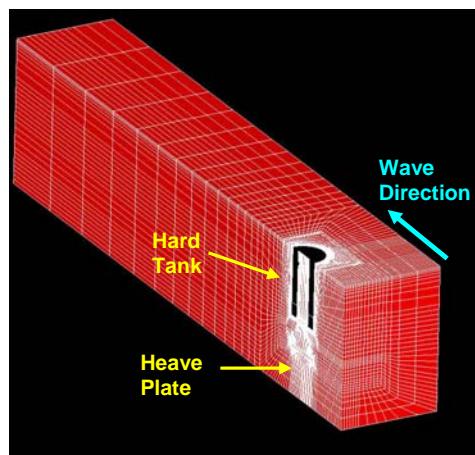
In this study we first simulate a baseline design in a moderate seastate in 1:60 scale assuming Froude scaling. The case chosen was a nominal full-scale single component wave with a height of 13.1 m with 15 second wave period. This results in a wave length of about 350 m or about 7 times the platform diameter. This case corresponds to a 1:60-scale model test that was previously modeled in a physical wave tank. We simulated both the 1:60 scale model test and the full-scale Spar platform geometry in order to estimate the effects of scaling, especially the scaling effect on the centerwell surface oscillations. Following these simulations, additional simulations were completed with more restrictive plate geometries in full scale to examine the effect of plate designs with reduced open areas which would limit centerwell water oscillations. These simulations were made modeling a 21.6m wave height, with a 15-second period and a 29.3m wave height with a 16 second period.

In the following sections we first describe the numerical method used in the simulations. We then describe the plate geometries chosen for the simulations and give examples of the simulation results. Data from the simulations are compared to corresponding data from model basin experiments. Scaling effects are estimated by comparing simulations of model scale and full scale flows. Finally, recommendations are made for future application of the methods developed here.

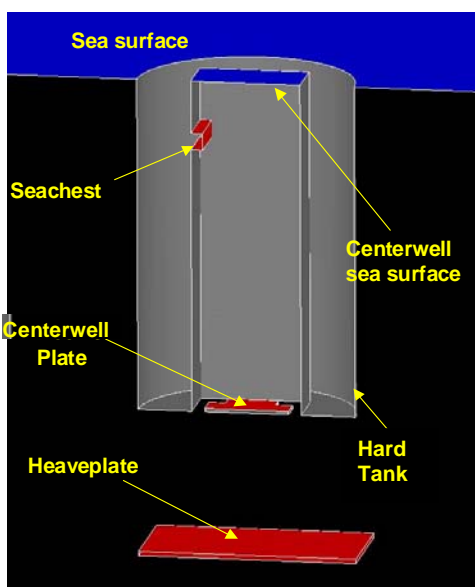
APPROACH

All of the solutions shown here were produced using the AcuSolve™ finite element CFD solver. AcuSolve is based on the Galerkin/Least-Squares formulation and supports a variety of element types. AcuSolve uses a fully coupled pressure/velocity iterative solver plus a generalized alpha method as a semi-discrete time stepping algorithm. AcuSolve is second order accurate in space and time. All of the solutions used an unsteady Reynolds averaged Navier-Stokes (URANS) turbulence model with the Spalart-Allmaras turbulence model [2]. Wall functions are used instead of resolving the boundary layer flow to the wall. The modeling approach is described in somewhat greater detail in [3] along with several other

references. Changes in the fluid domain shape due to waves are accommodated using arbitrary Lagrangian-Eulerian (ALE) mesh technology.



(a)



(b)

Figure 2. Surface mesh of fluid domain (top) and hard tank geometry (bottom)

It was felt from the onset that it might be necessary to model the flow field introduced by the waves passing the platform along with the platform motions in order to predict the fluid motions in the centerwell. Thus it was decided to model the waves by creating a fluid domain around the Spar hard tank and adding a free surface along with the gravity body force. The

uppermost heave plate is also included in the geometry as it was thought that the presence of this plate might influence the flow field near the centerwell opening, the vortex structure around the spar locally near the centerwell opening and hence the fluid flow in the centerwell. The Spar is aligned such that the centerwell plate and heave plate are symmetric about the mid-plane of the Spar in the wave direction so this was defined as a symmetry plane in order to reduce simulation size. The resulting meshes for the various geometries each contained about 250,000 nodes. A typical mesh is shown in Figure 2a and 2b. Note that the waves are generated at the inlet or right end of the mesh near the Spar. The mesh density at the outlet end of the mesh is low with a gradually increasing mesh length in the wave direction in order to damp out the waves and reduce reflections from the far end of the mesh. As shown in Figure 2b, the geometry includes the centerwell and plate, and a “seachest.” The seachest is a submerged manifold that distributes cold water piped from deep at the Spar keel to different cooling systems in the platform’s Topsides. Loads on the seachest were also calculated in this study but are not reported here.

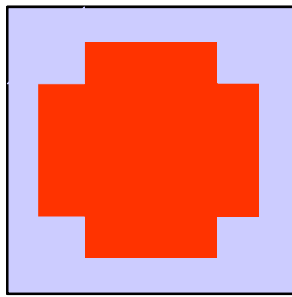
Comment [M1]: Not sure what this means? Please clarify.

Three configurations were used for the centerwell plate closure representing blockage ratios of 0.49, 0.71 and 0.85. The centerwell plate outlines are shown in Figure 3. Here the square is the outline of the centerwell opening and the blue zones are open to the sea while the red, green or yellow zones are the centerwell plate configurations. All three centerwells are open to the atmosphere at the top. Using the three geometries, a total of seven simulations were completed as shown in Table 1. In each case, the seastate contains only a single wave component. The 21.6m sea represents a 100 year event and the 29.3m sea represents a 1,000 year event.

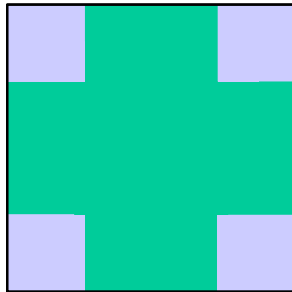
Deleted: 71ft

Deleted: 96ft

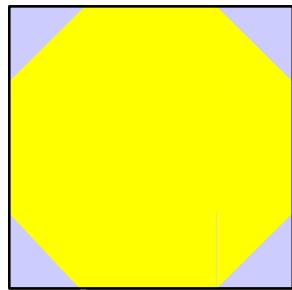
In each simulation, the waves were generated at the inlet surface by specifying the horizontal particle velocity as a function of depth and time. Tests with a mesh of the sea only (without the Spar) showed that this produced a sinusoidal wave in the fluid domain in the vicinity of the Spar. In simulations including the Spar geometry, the small Spar heave motions were specified as a function of time rather than calculated from the forces on the Spar. The phase angle and amplitude of heave were estimated from scale model experiments. Spar surge and sway were not modeled. Each simulation was run until the response of the fluid in the centerwell appeared to be periodic and then the simulation was run for an additional period corresponding to at least 10 wave periods. The time step used for the simulations was 0.25s full scale and 0.033s in 1:60 scale.



(a) Design 1, 49% Closure



(b) Design 2, 71% Closure



(c) Design 3, 85% Closure

Figure 3. Centerwell Plate Configurations

Table 1. Simulation Matrix

Wave Height*	CONFIGURATION			
	Design 1	Design 2	Design 3	Design 1 1:60 scale
13.1m	X	X	X	X
21.6m	X	X		
29.3m		X		

*Wave period is 15s for 13.1m and 21.6m seas and 16s for 29.3m sea.

TYPICAL RESULTS

Figure 4 shows the deformed mesh in a typical simulation. Note the difference in elevation of the centerwell free surface and the surrounding sea surface. The velocity contours show an increase in velocity magnitude near the Spar and at locations between the Spar and the heave plate. Note that the ratio of Spar frontal area to inlet area or blockage for this mesh is about 8%. Figure 5 shows the vertical motions of the sea surface at the Spar, the imposed heave motion, based on the model test data and the centerwell interior water surface motions. The example shown is for the centerwell plate Design 2 (see Figure 3) plate coverage but is typical of all of the designs. As shown in the figure, the heave motion is about 10% of the wave motion outside the Spar and has a phase lag near 90 degrees. The centerwell water elevation lags the exterior wave by about 6 seconds or a phase angle of 150 degrees. The motion of the fluid in the centerwell is reminiscent of an underdamped simple harmonic oscillator which is excited at a frequency greater than its natural frequency.

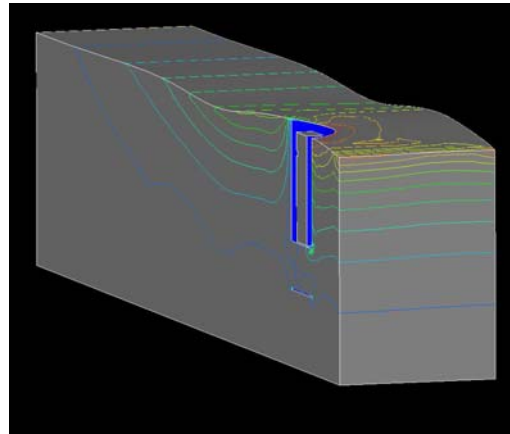


Figure 4. Deformed mesh with velocity magnitude contours

The vertical force on the centerwell plate and the load distribution were determined for each simulation. An example of the total force variation with time is shown in Figure 6 (positive upwards). The maximum load is relatively moderate for this configuration and this seastate and poses no particular problems for structural design. The load distribution on the centerwell plate was also found for each seastate and plate design. The total load and pressure distribution vary with time. Only a sample distribution is given here in Figure 7. This figure plots the net pressure load (upward) as a function of the distance from the centerline of the Spar in the wave propagation or in-line direction (x) and the cross flow direction (y). The plot is made at a time of maximum load and is noteworthy in that it shows a significant variation in the wave propagation direction. Thus it would appear that simple calculations based on the static head can produce large errors in load distribution over the plate.

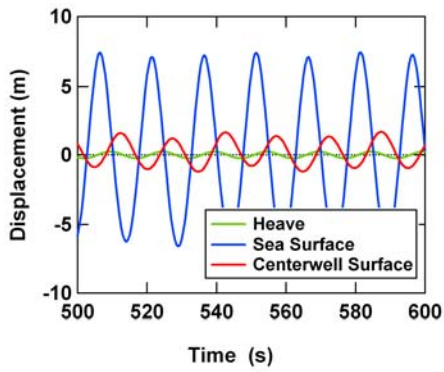


Figure 5. Vertical displacements of sea surface, centerwell water column height and Spar heave (Design 2 – 13.1m seas)

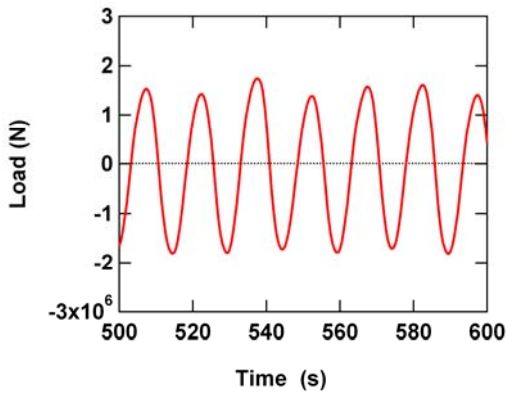


Figure 6. Vertical force (Design 2 – 13.1m wave height)

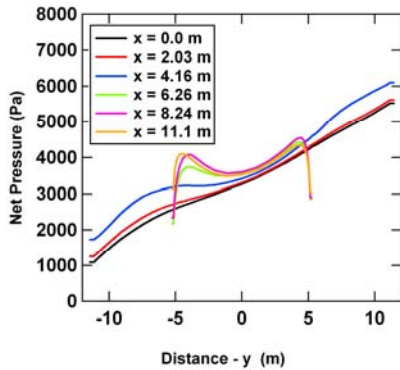


Figure 7. Load distribution on the centerwell plate at a time of maximum load, Design 2

Finally, we examined the spectra of the exterior sea wave elevations and the centerwell water surface motions to see if they provided any further information about the simulations. An example of this data is shown in Figure 8. The spectrum of the waves generated around the Spar (blue curve) in the simulation are dominated by the fundamental wave frequency (0.0665 Hz) corresponding to a wave period of 15s. Two harmonics of this frequency are also visible in the spectrum. The small peaks appearing below the fundamental wave frequency seem to be the result of reflections from the boundaries of the fluid domain. Finally, the spectrum of the centerwell surface (red curve) show similar harmonics with reduced amplitudes.

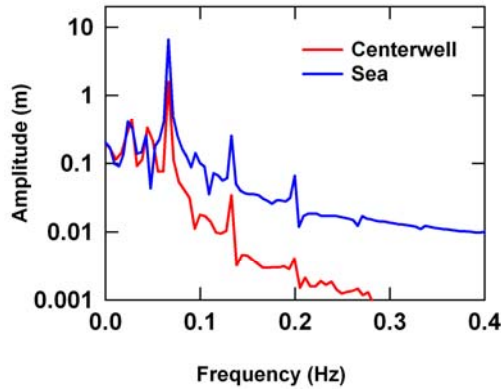


Figure 8. Amplitude spectra for external sea waves and centerwell water motions.

COMPARISON WITH MODEL EXPERIMENTS

An important part of this study was a comparison with model basin experiments in 1:60- scale. There are two objectives here. The first is to estimate the effect of scale factor so the model experiments could be confidently extrapolated to full scale and the second was to validate, if possible, the CFD simulations so that the loads distributions could be used for design purposes. In the model basin experiments both the centerwell surface motion and the total load on the centerwell plate were measured so these two parameters are used to test the CFD simulations. We estimated the effect of scaling directly by comparing CFD simulations of model scale experiments with similar CFD simulations for full scale operation based on the same Spar geometry and time scales and other boundary conditions based on Froude scaling. In general, the simulation showed that the model basin experiments should produce similar results to the full scale. In general, however, it was found that the full scale simulations predicted an overall increase in centerwell water motions of about 15% over that seen in the model scale simulations.

Table 2 compares the predicted centerwell surface motion height with the estimated motion height from the data measured

Deleted: amplitude

Deleted: amplitude

in model basin experiments. The data presented is based on adjacent maximum-minimum values for the baseline centerwell plate design. Note that the model results are projected to full scale in each case. Also, the CFD simulations were predictions so the wave heights in the model experiments are not exactly the same as those used for the CFD simulations. The realized wave heights are shown in each case to help in comparing the results. The associated full-scale centerwell plate loads are also shown for those cases where direct comparison is possible. As shown in the table the CFD simulations anticipate the extrapolated results from the model basin experiments pretty well. A direct comparison is given at the top of the table as the model experiments are simulated directly in this case.

Table 2. Comparison of CFD and Model Basin experiments

	Wave Height (m)	Centerwell Water Motion Height h (m) max-min		F (N) max-min	
		Exp.	CFD	Exp.	CFD
Experiment	14.1	3.8		2.3e6	
CFD 1:60	13.1		3.5		3.0e6
Experiment	14.1	3.8		2.3e6	
CFD - FS	13.1		4.0		2.3e6

Here, the measured model basin wave height is 14.1m while the CFD solution produced 13.1m. However, the CFD solution predicted slightly lower centerwell water motion heights and higher forces. This may be due to the mesh resolution used here but it should also be noted that the reported model test results are for the relative motions, measured by a wave probe mounted on the model, and the comparisons are not exactly one to one with the calculated centerwell motions, since they contain a small component of Spar heave.

The CFD simulation at full scale predicts an increase in maximum centerwell water motion height of 0.5m (15%) above that predicted in model scale and a decrease in load amplitude of 23% from that predicted for model scale. These suggest a significant scaling effect. As discussed earlier, we expect that the large eddy structure around the spar may influence the flow locally near the opening and therefore in and out of the centerwell. This may cause a scaling effect in addition to expected changes in the discharge coefficient for the plate openings.

RESULTS

The series of simulations outlined in Table 1 was run to determine the effect of seawater centerwell plate blockage ratio on the centerwell water surface motions and the loads on the centerwell plate. All of the simulations were run in full scale as described earlier. The results of these simulations are summarized in Table 3. These data show that centerwell wave height can be controlled effectively by increasing blockage at a cost of increased loading on the centerwell plate. In particular, increasing the blockage while keeping the wave height constant at 13.1m decreased the centerwell max minus min height by 60% while the max minus min centerwell plate load increased by a factor of three.

The data also indicate that centerwell wave motions are roughly proportional to the height of the external waves for this single component wave case as shown by the data for Design 2. The centerwell plate loads in this case, however, increase roughly as the square of the external wave height indicating that simple estimates based on the implied static head based on the wave height should not be used for design purposes.

Table 3. Centerwell Water Motion Height and Centerwell Plate Load (max-min)

Wave Height	Configuration		
	Design 1	Design 2	Design 3
Blockage Ratio	0.49	0.71	0.85
13.1m	4.0 m 2.3e6 N	3.0 m 4.1e6 N	1.6 m 7.1e6 N
21.6m	5.8 m 4.1e6 N	4.4 m 9.5e6	-
29.3m	-	7.0 m 2.2e7 N	-

The data shown in Tables 2 and 3 are plotted in Figures 9 and 10 to better show the effects of scaling and of blockage on wave height and centerwell plate load. As shown, the centerwell wave height is roughly proportional to the external wave height as is the maximum plate load. The data also show that the centerwell wave height is effectively reduced by increasing the centerwell plate blockage ratio, but also that centerwell plate loads increase rapidly as well.

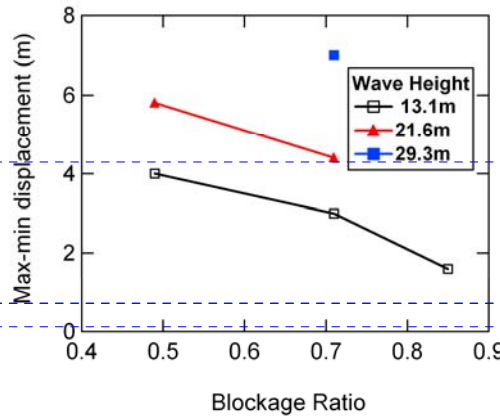


Figure 9. Centerwell wave height vs. blockage ratio

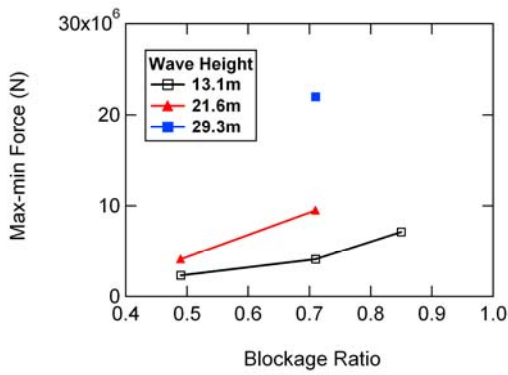


Figure 10. Maximum total centerwell plate load vs. blockage ratio

COMPARISON WITH INCIDENT WAVES

In linear potential theory, in deep water the incident wave particle motions decay exponentially with depth. In the absence of any disturbance from the hull, the wave particle motion height (peak to trough) at the bottom of the centerwell h would be

$$h = H e^{-kz}$$

where,

H = Height of the incident wave at the exterior free surface,

$$k = \frac{\omega^2}{g}$$

is the wave number,

$$\omega = \frac{2\pi}{T}$$

z is the depth at the bottom of the centerwell, and

T is the wave period

If the centerwell bottom was completely open (no centerwell plate), and if there were no heave or disturbance effects from the hard tank or heave plates, the centerwell water motion could be thought of as essentially driven by the incident wave particle motion at its bottom. Then, the centerwell water motion heights would be the same as those at the centerwell bottom given in Table 4 below:

Table 4. Incident wave particle motion heights at the bottom of the centerwell (max-min)

Wave Height H (m)	Period (s)	Particle motion height at centerwell bottom (m)
13.1	15	3.6
21.6	15	6.0
29.3	16	9.5

Although the realistic situation is much more complex, the calculated heights of centerwell water motions given in Table 3

are indeed quite similar to the wave particle motions at the bottom of the centerwell given in Table 4 above. These are also quite similar to the relative motion results given in Table 2 above. It appears that this small 49% closure configuration is not sufficient to damp out the water motions in the centerwell. The centerwell water motion height for Design 1 is essentially the same as the incident wave particle motion height at the bottom of the centerwell.

For Designs 2 and 3, as the closure ratio increases, there is a clear reduction of the centerwell water motion height compared to the motion of the incident wave at the centerwell bottom given in Table 4. As expected, the loads on the plate also increase as the closure ratio increases.

SPAR HEAVE MOTIONS

In these CFD simulations, the Spar motions were not solved as a function of the forces on the platform, but to save computation and turn-around time, were imposed based on the model tests for the available (most open) centerwell plate. This gave sufficient information for design of the centerwell plate and assurance the centerwell water motions would remain sufficiently small at full scale. However, the forces on the centerwell plate shown above increase with increasing closure and this might influence the heave motions of the Spar.

Note that a Spar is usually designed to have small heave motions for a given set of environment conditions. This is achieved by a combination of low exciting force, a long natural period in heave and sufficient damping. The resulting heave motions are typically much smaller than the exterior sea surface or incident wave motion, except at very long periods, where the incident wave heights are small.

The heave exciting force for a Spar is kept relatively small by making the hard tank sufficiently deep and slender. In potential theory, the pressures due to the incident wave decay exponentially with depth, similar to the above discussion on wave particle motions. The combination of small area and small pressure means the total heave exciting force remains small. The natural period in heave is typically made longer than the majority of the energy in the incident wave spectrum. This is achieved through the use of heave plates which provide added mass. The heave plates also provide viscous damping which due to its non-linear behavior becomes especially effective when motions start to increase.

ADDITIONAL MODEL TEST RESULTS

To confirm that the heave motions and Spar centerwell water motions remain small for higher centerwell plate closures, results from additional model tests are presented. These results are taken from model tests of a similar Spar with a centerwell closure of about 78%.

Vertical relative motions were measured at two points in the centerwell using wave probes attached to the model. One probe was attached at the centerline of the centerwell (RELM CW CL) and the other near the corner of the centerwell (RELM CW NW).

Formatted: Font: Times New Roman, 10 pt

Figure 11 and Figure 12 show the Response Amplitude Operators (RAOs) for heave and vertical relative motions in the centerwell. The RAO is defined as the amplitude of the response divided by the incident wave amplitude at the same frequency. As opposed to the results presented above for waves of a single frequency, these cases are for irregular seas comprising a wave spectrum. Two cases are shown, for a small and a large seastate, respectively. The seastates are characterized by the significant wave height H_s , and the spectral peak period, T_p . Figure 13 shows the power spectra in the large seastate case, which represents a severe Gulf of Mexico hurricane. The small seastate is a small-amplitude, wide-band spectrum, useful for obtaining RAOs over a wide range of frequencies in a single experiment.

The following observations are made looking at the figures:

1. The first lateral sloshing mode is clearly visible as a spike in the relative motion RAO near 4.25 seconds. It shows up mainly at the corner Relative motion probe, since this mode has a maximum at the edge of the centerwell and a minimum at the centerline. Higher modes are also present in the response. However, these are not significant, since there is little energy.
2. Comparing the RAOs in the small and large seastates, both the heave and relative motion RAOs depend strongly on wave amplitude. Thus, the concept of an RAO is not entirely appropriate. An RAO that depends on the seastate cannot readily be applied at other seastates. However, such RAOs are useful in comparing the magnitude of responses in different seastates to assess non-linear effects.
3. Viscous forces are at work, both on heave motions and the centerwell water motions. The small seastate heave RAO contains a resonant peak at the natural period of 21.5 seconds, while in the large seastate, this peak is nearly absent and the RAO barely reaches 1.0. The difference is due to the effects of heave plate damping, which is appropriately modeled using Morison damping coefficients in the time domain.
4. For centerwell water motion RAOs, there is an even greater reduction, from about 2.5 in the small seastate to well below 1.0 in the larger seastate. Potential flow methods are not expected to perform well without accounting for viscous damping effects, as water enters and leaves the centerwell through constrictions in the plating at the centerwell bottom.
5. For this Spar, the centerwell vertical motion natural period is near 16 seconds, whereas the highest relative motion RAOs occurs for longer periods than this (18s and 18-21s, for small and large seastates, respectively). The behavior around these periods does not show any unusual effects.

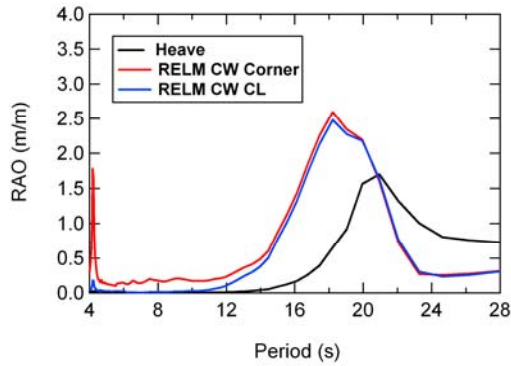


Figure 11. RAOs of heave and vertical relative motions at two points in the centerwell, small seastate (wide-band spectrum, $H_s=3.25\text{m}$).

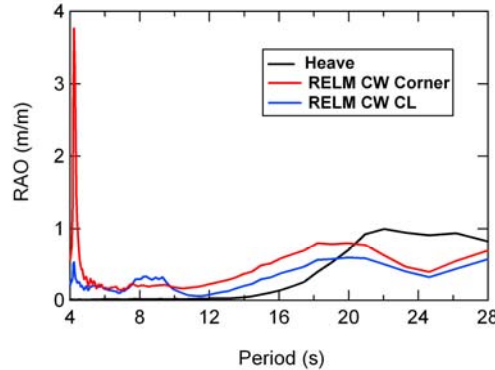


Figure 12. RAOs of heave and vertical relative motions at two points in the centerwell, large seastate, ($H_s=15.6\text{m}$, $T_p=15.8\text{s}$).

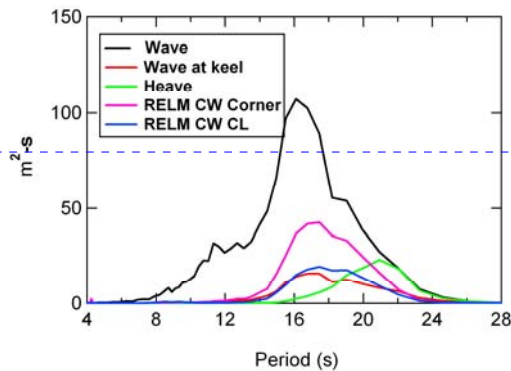


Figure 13. Power spectral densities of waves, heave and vertical relative motions at two points in the centerwell, large seastate, ($H_s=15.6\text{m}$, $T_p=15.8\text{s}$).

Deleted: (Deck 3)

CONCLUSIONS

A series of CFD simulations were made to supplement model basin experiments in the design of a centerwell plate at the bottom of a hard tank. The purpose of the study was to design a centerwell plate with the appropriate blockage that would control centerwell water surface motions but not create excessive loads on the centerwell plate. A comparison of predicted centerwell motions and plate loads for baseline experiments showed reasonable agreement although the external wave heights were not exactly the same for the two cases. Adjustment for this effect suggests that the CFD simulations at the scale of the model underpredict the centerwell motions and overpredict the plate loads. By comparing simulations at model scale (1:60) and full scale we concluded that there is a scaling effect of about 15% in the centerwell wave height. [Based on previous studies, this result is not unexpected, but should be confirmed by further analysis and if possible, full-scale data.](#)

An additional series of simulations was completed in which the seastate and blockage of the centerwell plate were varied. The results of these simulations show that centerwell motions can be effectively damped by increasing the centerwell blockage ratio. However, the maximum centerwell plate loads also increased rapidly. There appears to be an optimum range of blockage ratios which provides adequate damping of the centerwell motions without creating excessive loads on the centerwell plate.

This study also suggests that relatively simple CFD simulations can be used in the design of the centerwell plate and associated structures. Additional model test results show that while the RAOs may appear large in small seastates, both the heave and centerwell water motions remain small in the all-important large Gulf of Mexico hurricanes.

REFERENCES

1. Chiu Y. H. and Etheridge, D.W., "External flow effects on the discharge coefficients of two types of ventilation opening," J. Wind Engineering and Industrial Aerodynamics, Vol. 95, Issue 4, April 2007, pp. 225-252
2. Spalart, P. R. and S. R. Allmaras, "A one-equation model for aerodynamic flows," AIAA 92-0439 (1992)
3. Oakley, O.H. Constantinides, Y., Navarro, C. and Homes, S. "Modeling vortex induced motions of spars in uniform and stratified flows," OMAE2005-67238

Deleted: ¶

¶

Formatted: Indent: Left: 0 pt,
Tabs: 18 pt, List tab + Not at 36 pt